Dynamic reflectionless defects in tight-binding lattices

Stefano Longhi and Giuseppe Della Valle
Dipartimento di Fisica, Politecnico di Milano, Piazza L. da Vinci 32, I-20133 Milano, Italy
(Received 17 October 2011; revised manuscript received 11 November 2011; published 21 November 2011)

In tight-binding lattices, localized modes are generally created by the introduction of structural impurities in the otherwise homogeneous lattice. In most cases, impurities are not transparent and cause scattering (reflection) of Bloch wave packets. Here it is shown that the application of high-frequency and strong ac fields in a certain class of lattices with structural impurities can make them reflectionless, yet preserving their localization properties. Hence, a structural defect in the lattice supporting a localized mode, which is a scattering center when the external ac field is switched off, can be dynamically transformed into a reflectionless defect when the external field is switched on.

DOI: 10.1103/PhysRevB.84.193105 PACS number(s): 73.23.−b, 72.15.Rn, 63.20.Pw, 42.82.Et

Propagation, scattering, and localization phenomena in tight-binding lattices with inhomogeneities is a subject of continuous interest in different areas of physics. Structural[1–3] or nonlinearly induced[4] defects, disorder,[1] or local coupling channels[5] are responsible for important physical effects, such as resonant scattering, Anderson localization, and Fano resonances (see, for instance, Ref. 6, and references therein). The application of strong ac fields can deeply modify the transport, localization, and scattering properties of both homogeneous and inhomogeneous lattices. In homogeneous lattices, ac driving with a suitable ratio between the amplitude and the frequency of forcing can lead to the suppression of diffusion of a particle wave packet, which undergoes periodical self imaging of its initial distribution. Such a phenomenon, originally predicted by Dunlap and Kenkre[7] and referred to as dynamic localization, is related to the collapse of the quasienergy band of the periodically driven lattice[8] and has been recently observed for cold atoms and Bose-Einstein condensates in periodically shaken optical lattices[9] and for light waves in periodically curved optical waveguide arrays.[10] Ac-driving is also an efficient tool to control the scattering and localization properties of inhomogeneous lattices.[11–21] For example, it has been shown that an ac field can control the localization length of a defect mode supported by a single impurity,[12] the tunneling between two communicating defects,[17] the number of surface states in truncated lattices,[20] and the localization-delocalization transition in disordered lattices.[13,18,19] An ac field can be also exploited to clean impurities and potential barriers, making the lattice effectively homogeneous.[16,21] Most of such phenomena are basically related to renormalization of the effective hopping rate between adjacent sites in the lattice induced by the ac field.

The simplest way to create localized states in a homogeneous lattice is the introduction of structural impurities in one or more lattice sites. In most cases, such impurities, besides introducing localized (defect) modes with energies in the gap, cause a Bloch wave packet propagating in the lattice to be scattered off, i.e., to be partially reflected at the impurity sites. However, there exist some special structural inhomogenities supporting localized modes that are *reflectionless*, i.e., that appear to be transparent to Bloch wave packets.[25–28] Structural reflectionless impurities on a lattice, which support an arbitrary number of localized states, can be synthesized in a rather general way by use of the Darboux transformation of supersymmetric quantum mechanics.[25,27] An experimental demonstration of such a kind of structural reflectionless inhomogeneities on a lattice has been recently reported by Szameit and collaborators[28] in femtosecond-laser-written photonic lattices with controlled waveguide spacing. In this Brief Report we propose *dynamic* reflectionless impurities on a lattice, i.e., impurities sustaining localized states that are not reflectionless but that can be done so when a strong ac field, with appropriate amplitude and frequency, is applied. Hence, switching on or off an external field can make a localized defect transparent or opaque to Bloch wave packets.

Let us consider the tight-binding system shown in Fig. 1(a), driven by an external sinusoidal field $E_x(t) = E_0 \cos(\omega t)$ applied along the x axis. The lattice comprises three impurities at the sites $n = 0$ and $n = \pm 1$. In the tight-binding approximation and considering only tunneling between nearest neighboring, the single-particle Hamiltonian of the system reads

$$\hat{H} = -\hbar\kappa \sum_n (|n\rangle\langle n+1| + |n+1\rangle\langle n|) + \sum_n [\hbar\epsilon_n + x_n e E_x(t)]\,|n\rangle\langle n|, \tag{1}$$

where $|n\rangle$ is the Wannier state localized at the n-th site of the lattice with energy $\hbar\epsilon_n$, κ is the hopping rate between adjacent sites, and x_n is the x-coordinate of the n-th site. For the arrangement of Fig. 1(a), the values of ϵ_n and x_n read explicitly

$$\epsilon_n = \begin{cases} 0 & \text{for} \quad |n| \geqslant 2 \\ \sigma & \text{for} \quad n = \pm 1 \\ U & \text{for} \quad n = 0 \end{cases} \tag{2}$$

and

$$x_n = \begin{cases} (n+1)a & \text{for} \quad |n| \leqslant -2 \\ 0 & \text{for} \quad n = 0, \pm 1 \\ (n-1)a & \text{for} \quad n \geqslant 2, \end{cases} \tag{3}$$

where a is the separation between adjacent sites in the lattice. If the state vector $|\psi(t)\rangle$ of the system is decomposed on the Wanner basis as $|\psi(t)\rangle = \sum_n c_n(t)|n\rangle$, the evolution of

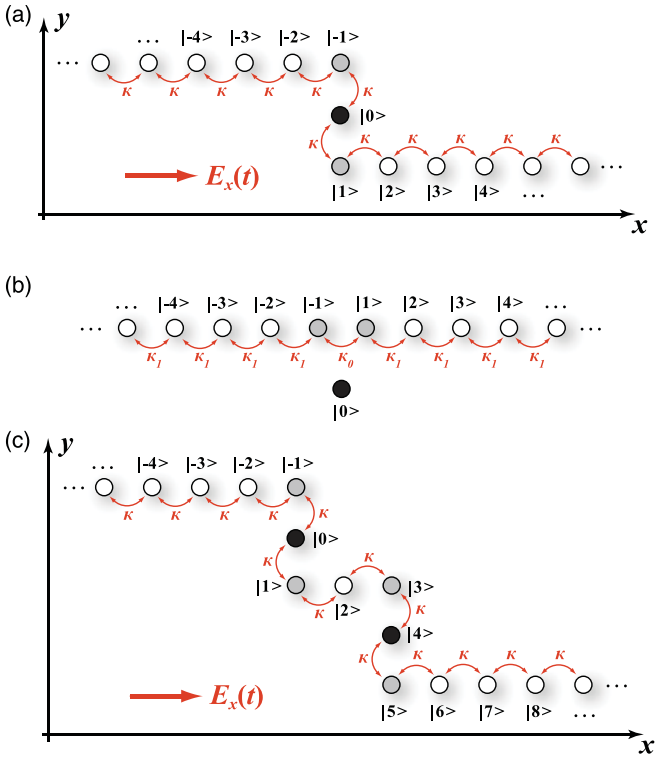

FIG. 1. (Color online) (a) Schematic of an ac-driven tight-binding lattice with uniform hopping amplitudes κ comprising one strong ($|U| \gg \kappa$) and two weak ($|\sigma| \ll \kappa$) impurities at sites $n = 0$ and $n = \pm 1$, respectively. (b) Effective lattice model, obtained by asymptotic analysis of Eq. (4), in which the strong impurity is decoupled from the lattice. (c) Schematic of an ac-driven tight-binding lattice, comprising two strong and four weak impurities, obtained by cascading the building block of Fig. 1(a).

the probability amplitudes c_n describing the occupation of the various sites in the lattice is governed by the coupled equations

$$i\frac{dc_n}{dt} = -\kappa(c_{n+1} + c_{n-1}) + [\epsilon_n + eE_x(t)x_n/\hbar]\,c_n. \qquad (4)$$

The tight-binding Hamiltonian Eq. (1), with controlled site energies as dictated by Eq. (2), can be implemented in different physical systems. For example, Eq. (1) can describe the coherent single-electron dynamics in mesoscopic systems,[22,23] such as in an ac-driven chain of coupled quantum dots in the geometrical setting of Fig. 1(a), in which the energies ϵ_n at lattice sites $n = 0, \pm 1$ can be controlled by dc gate potentials. Similarly, Eq. (4) can describe light transport in an array of evanescently coupled optical waveguides with a sinusoidally curved optical axis, in which the periodic axis bending mimics the effect of an ac field and the site energies ϵ_n define the propagation constants of the modes trapped in the various waveguides.[24] In this optical system, tailoring of ϵ_n, as requested by Eq. (2), can be achieved by varying either the refractive index change or the core size of the waveguides at lattice sites $n = 0, \pm 1$. In the absence of the external driving field (i.e., for $E_x = 0$) and far from the defect region, a Bloch wave packet with carrier momentum p propagates along the lattice with a group velocity $v_{g1} = 2\kappa a \sin(pa)$. As the wave packet reaches the defect region near $n = 0$, it is scattered off owing to the impurities at the lattice sites $n = 0, \pm 1$. We

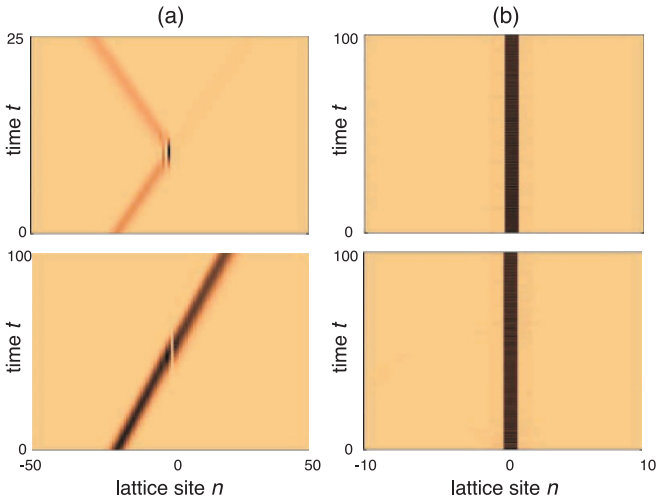

FIG. 2. (Color online) Snapshots of occupation probabilities $|c_n(t)|^2$ versus time in the tight-binding lattice of Fig. 1(a) for parameter values $\kappa = 1$, $U = 5$, $\sigma = 0.2$, $\omega = 4$, $\Gamma = 2.0415$ and for the ac driving field switched off (upper panels) and on (lower panels). The panels in (a) correspond to Bloch wave packet excitation $c_n(0) \propto \exp[-(n - n_0)^2/w^2 + iapn]$ with offset $n_0 = -20$, wave packet width $w = 4$, and momentum $p = \pi/(2a)$, whereas panels (b) correspond to the initial particle localized at the $n = 0$ site, i.e., $c_n(0) = \delta_{n,0}$.

typically consider the case of a strong impurity at the site $n = 0$, $|U| \gg \kappa$, and a weak impurity at the sites $n = \pm 1$, $|\sigma| \ll \kappa$. In this case, the lattice sustains a single localized mode near $n = 0$, and the impurity at $n = 0$ is fully opaque, i.e., a Bloch wave packet incident onto it is almost completely reflected, as shown in the upper panel of Fig. 2(a). Our aim is to make the impurity transparent to Bloch wave packets by application of a strong ac field, without destroying the localization property of the impurity. To this aim, it is worth introducing the new amplitudes a_n according to

$$c_n = a_n \exp\left[-i\frac{\Gamma x_n}{a}\sin(\omega t) - iU\delta_{n,0}t\right] \qquad (5)$$

and the normalized time variable $\tau = Ut$, where $\Gamma = eaE_0/(\hbar\omega)$; in this way, Eq. (4) takes the form

$$i\frac{da_n}{d\tau} = (\epsilon_n/U - \delta_{n,0})a_n - \frac{\kappa}{U}a_{n+1}\exp[i\Phi_{n+1}(t)] - \frac{\kappa}{U}a_{n-1}\exp[-i\Phi_n(\tau)], \qquad (6)$$

where we have set $\Phi_n(\tau) \equiv (\Gamma/a)(x_{n-1} - x_n)\sin(\omega\tau/U) + (\delta_{n-1,0} - \delta_{n,0})\tau$. Equation (6) is suited for a multiple-time scale asymptotic analysis.[29] Here we assume κ/U as a small parameter—of order, say, $\sim \epsilon$—with the scaling $\omega/U \sim 1$, $\sigma/U \sim \epsilon^2$, and $J_0(\Gamma) \sim \epsilon$, where J_0 is the zero-order Bessel function of first kind. The last condition corresponds to a choice of the ac driving amplitude and frequency close to the dynamic localization regime.[7] Moreover, the ratio ω/U is assumed to be far from any integer number to avoid resonance effects. The solution to Eq. (6) is searched as a power series $a_n = a_n^{(0)} + \epsilon a_n^{(1)} + \epsilon^2 a_n^{(2)} + \ldots$, and multiple time scales $T_0 = \tau$, $T_1 = \epsilon\tau$, $T_2 = \epsilon^2\tau, \ldots$ are introduced to remove secular growing terms at various orders in the

asymptotic analysis. Using the derivative rule $d/d\tau = d/dT_0 + \epsilon d/dT_1 + \epsilon^2 d/dT_2 + ...$ in Eq. (6), a hierarchy of equations for successive corrections to a_n are obtained by equating the terms of the same order in ϵ. At leading order $\sim \epsilon^0$, one simply obtains $\partial_{T_0} a_n^{(0)} = 0$, i.e.,

$$a_n^{(0)} = A_n(T_1, T_2, ...), \tag{7}$$

where the amplitudes A_n vary on the slow time scales $T_1, T_2, ...$. The evolutions of the amplitudes A_n on the slow time scales T_1, T_2,... are obtained from the solvability conditions at the various orders $\epsilon, \epsilon^2, ...$[29]. At order $\sim \epsilon$, one obtains $\partial_{T_1} A_n = 0$, whereas at order ϵ^2 the solvability conditions yield

$$iU\frac{dA_n}{dT_2} = -\kappa_1(A_{n+1} + A_{n-1}) \quad |n| \geqslant 2, \tag{8}$$

$$iU\frac{dA_{-1}}{dT_2} = -\kappa_1 A_{-2} - \kappa_0 A_1 - \rho A_{-1}, \tag{9}$$

$$iU\frac{dA_1}{dT_2} = -\kappa_1 A_2 - \kappa_0 A_{-1} - \rho A_1, \tag{10}$$

$$iU\frac{dA_0}{dT_2} = 0, \tag{11}$$

where we have set $\kappa_1 = \kappa J_0(\Gamma)$, $\kappa_0 = \kappa^2/U$, and $\rho = \sigma - \kappa_0$. If we stop the analysis at this order, the leading-order approximate solution to Eq. (4) is thus given by Eqs. (5) and (7), where the slow evolution of amplitudes A_n in the physical time variable t is governed by Eqs. (8)–(11), with the replacement $U(d/dT_2) \to d/dt$. Hence, the application of the strong ac field basically transforms the original tight-binding lattice of Fig. 1(a) into the effective lattice shown in Fig. 1(b), in which the strong impurity at site $|0\rangle$ is effectively decoupled from the lattice. The tunneling from the sites $n = -1$ and $n = 1$, with a hopping amplitude κ_0, is a second-order process, which is accompanied by a shift of the site energies by $-\kappa_0$. The reduction of the hopping rate between the other lattice sites, from κ to κ_1, is the usual hopping renormalization induced by an ac field.[7,8] Remarkably, if the amplitude E_0 and frequency ω of forcing are chosen such that $\kappa_1 = \kappa_0$ and the weak impurity σ such that $\rho = 0$, i.e., if the following conditions are satisfied:

$$J_0(eaE_0/\hbar\omega) = \kappa/U, \quad \sigma = \kappa^2/U, \tag{12}$$

it follows that the effective lattice, composed by the sites ..., $|-3\rangle, |-2\rangle, |-1\rangle, |1\rangle, |2\rangle, |3\rangle, ...$ turns out to be *homogeneous* (i.e., defect-free) and, thus, Bloch waves are not scattered off and propagate along the effective lattice with a reduced group velocity $v_{g2} = (\kappa/U)v_{g1}$. This is shown, as an example, in the lower panel of Fig. 2(a), where the propagation of a Bloch wave packet, as obtained by numerical integration of Eq. (4), using an accurate variable-step fourth-order Runge-Kutta method, is shown in the ac-driven lattice for parameter values satisfying the conditions of Eq. (12). Note that, according to the asymptotic analysis, in the driven lattice the impurities are basically reflectionless. It should be noted that the effect of the ac field is *not* to clean the impurities of the original lattice, erasing the localized defect mode sustained by the strong impurity (a case which was previously investigated in Refs. 16 and 21), rather it is to decouple the strong impurity from the lattice. The persistence of the localized defect state

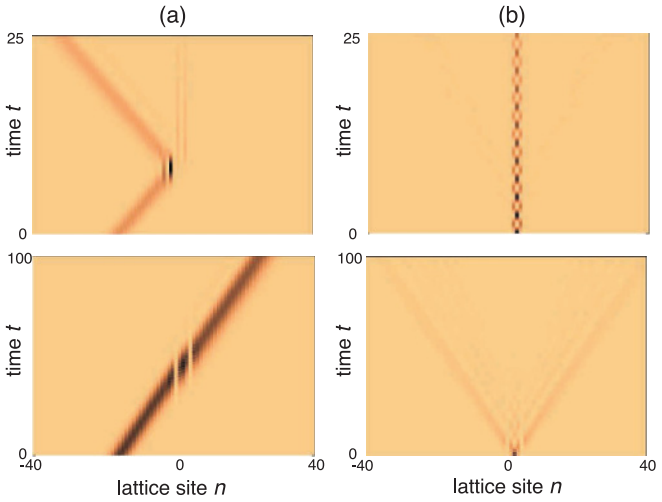

FIG. 3. (Color online) Snapshots of occupation probabilities $|c_n(t)|^2$ versus time in the tight-binding lattice of Fig. 1(c) for parameter values $\kappa = 1$, $U = 5$, $\sigma = 0.2$, $\omega = 4$, $\Gamma = 2.0415$ and for the ac driving field switched off (upper panels) and on (lower panels). The panels in (a) correspond to Bloch wave packet excitation $c_n(0) \propto \exp[-(n-n_0)^2/w^2 + iapn]$ with offset $n_0 = -15$, wave packet width $w = 4$, and momentum $p = \pi/(2a)$, whereas panels (b) correspond to the initial particle localized at the $n = 2$ site, i.e., $c_n(0) = \delta_{n,2}$.

is clearly shown in the bottom panel of Fig. 2(b), where the evolution of the site occupation probabilities are depicted for initial single-site excitation $c_n(0) = \delta_{n,0}$. Note that, for such an initial condition, the particle remains trapped at the strong impurity site, according to Eq. (11).

The idea to make a strong impurity in a lattice reflectionless by application of a suitable strong and high-frequency ac field can be extended to the case of multiple impurities by cascading the basic building block of Fig. 1(a). As an example, in Fig. 1(c) it is shown the schematic of a chain obtained by cascading two building blocks and comprising two strong impurities U at lattice sites $n = 0$ and $n = 4$, and four weak impurities σ at lattice sites $N = -1, 1, 3$, and 5. The propagation of a Bloch wave packet in this lattice, for the ac field switched off and on, is shown in the upper and lower panels of Fig. 3(a), respectively. Note that, when the ac field is switched on, the defects in the lattice become reflectionless, whereas for the ac field switched off the wave packet is mostly reflected, with some localization at the defects. It is interesting to examine the evolution of the site occupation probabilities for single-site excitation of the lattice at $n = 2$, i.e., for a particle initially localized between the two strong impurities [see Fig. 1(c)]. In the absence of the ac field [upper panel of Fig. 3(b)], the particle mostly remains localized between the two strong impurities at lattice sites $n = 0$ and $n = 4$. The periodic pattern observed in Fig. 3(b) is basically due to the beating of the two defect modes supported by the lattice of Fig. 1(c), which are symmetrically excited at $t = 0$. The slow decay of localization with time noticeable in the upper panel of Fig. 3(b) is due to the initial excitation of scattering (Bloch) states, which slowly radiate far from the defect region and correspond to a nonvanishing probability of the particle to tunnel the strong impurity sites. As the ac field is switched on, the evolution of the occupation probabilities is

shown in the lower plot of Fig. 3(b). In this case, the localized particle undergoes a ballistic motion like in a homogeneous lattice (see, for instance, Ref. 30), i.e., the impurities in the lattice appear to be reflectionless and do not trap anymore the particle between them. The scenario depicted in Fig. 3 can be obviously extended to a sequence of more than two impurities. Other lattice settings with structural impurities that become reflectionless under the application of an ac field could be envisaged as well. Finally, we would like to briefly mention that a possible experimental realization of the lattices shown in Fig. 1 is provided by light transport in engineered two-dimensional waveguide arrays, in which the ac driving field is mimicked by sinusoidal bending of the waveguide axis.[10]

In this Brief Report we have shown that application of high-frequency and strong ac fields in a certain class of lattices with structural impurities can make them reflectionless, yet preserving their localization properties. As compared to the phenomenon of field-induced defect transparency,[16,21] the ac driving field does not cancel the impurities in the lattice, rather it effectively decouples them from the homogeneous part of the lattice. This ensures that a Bloch wave packet is not scattered off by the impurities, and the localization states at the impurity sites are not destroyed by the ac field. Our results thus demonstrate the existence of *field-induced* reflectionless impurities in tight binding lattices, which are distinct from *structural* reflectionless lattice impurities recently predicted and experimentally observed in Refs. 26–28. Dynamic reflectionless impurities offer the rather important possibility to dynamically switch a strong scattering impurity from being opaque to being reflectionless.

The authors acknowledge financial support by the Italian MIUR (Grant No. PRIN-2008-YCAAK).

[1] A. A. Maradudin, *Theoretical and Experimental Aspects of the Effects of Point Defects and Disorder on the Vibrations of Crystals* (Academic Press, New York, 1966).
[2] P. Tong, B. Li, and B. Hu, Phys. Rev. B **59**, 8639 (1999).
[3] R. A. Suris and P. Lavallard, Phys. Rev. B **50**, 8875 (1994).
[4] G. P. Tsironis, M. I. Molina, and D. Hennig, Phys. Rev. E **50**, 2365 (1994); S. Flach, A. E. Miroshnichenko, V. Fleurov, and M. V. Fistul, Phys. Rev. Lett. **90**, 084101 (2003).
[5] A. E. Miroshnichenko, S. F. Mingaleev, S. Flach, and Yu. S. Kivshar, Phys. Rev. E **71**, 036626 (2005).
[6] A. E. Miroshnichenko, S. Flach, and Y. S. Kivshar, Rev. Mod. Phys. **82**, 2257 (2010).
[7] D. H. Dunlap and V. M. Kenkre, Phys. Rev. B **34**, 3625 (1986).
[8] M. Holthaus, Phys. Rev. Lett. **69**, 351 (1992).
[9] K. W. Madison, M. C. Fischer, R. B. Diener, Q. Niu, and M. G. Raizen, Phys. Rev. Lett. **81**, 5093 (1998); H. Lignier, C. Sias, D. Ciampini, Y. Singh, A. Zenesini, O. Morsch, and E. Arimondo, *ibid.* **99**, 220403 (2007); A. Eckardt, M. Holthaus, H. Lignier, A. Zenesini, D. Ciampini, O. Morsch, and E. Arimondo, Phys. Rev. A **79**, 013611 (2009).
[10] S. Longhi, M. Marangoni, M. Lobino, R. Ramponi, P. Laporta, E. Cianci, and V. Foglietti, Phys. Rev. Lett. **96**, 243901 (2006); A. Szameit, I. L. Garanovich, M. Heinrich, A. A. Sukhorukov, F. Dreisow, T. Pertsch, S. Nolte, A. Tünnermann, S. Longhi, and Y. S. Kivshar, *ibid.* **104**, 223903 (2010).
[11] D. H. Dunlap and V. M. Kenkre, Phys. Rev. B **37**, 6622 (1988).
[12] D. W. Hone and M. Holthaus, Phys. Rev. B **48**, 15123 (1993).
[13] M. Holthaus, G. H. Ristow, and D. W. Hone, Phys. Rev. Lett. **75**, 3914 (1995); Europhys. Lett. **32**, 241 (1995).
[14] J. Karczmarek, M. Stott, and M. Ivanov, Phys. Rev. A **60**, R4225 (1999).
[15] A. Z. Zhang, D. Suqing, X.-G. Zhao, and J.-Q. Liang, Physica B **291**, 275 (2000); A.-Z. Zhang, P. Zhang, D. Suqing, X.-G. Zhao, and J.-Q. Liang, Phys. Rev. B **63**, 045319 (2001).
[16] S. Longhi, Phys. Rev. B **73**, 193305 (2006).
[17] C. Weiss, Phys. Rev. B **73**, 054301 (2006).
[18] W. Zhang and S. E. Ulloa, Phys. Rev. B **74**, 115304 (2006).
[19] D. F. Martinez and R. A. Molina, Phys. Rev. B **73**, 073104 (2006).
[20] I. L. Garanovich, A. A. Sukhorukov, and Y. S. Kivshar, Phys. Rev. Lett. **100**, 203904 (2008); A. Szameit, I. L. Garanovich, M. Heinrich, A. A. Sukhorukov, F. Dreisow, T. Pertsch, S. Nolte, A. Tünnermann, and Y. S. Kivshar, *ibid.* **101**, 203902 (2008).
[21] S. Longhi, Phys. Rev. B **82**, 205123 (2010).
[22] S. Kohler, J. Lehmann, and P. Hänggi, Phys. Rep. **406**, 379 (2005).
[23] J. M. Villas-Boas, S. E. Ulloa, and N. Studart, Phys. Rev. B **70**, 041302(R) (2004); G. M. Nikolopoulos, D. Petrosyan, and P. Lambropoulos, Europhys. Lett. **65**, 297 (2004); D. Huang, S. K. Lyo, and G. Gumbs, Phys. Rev. B **79**, 155308 (2009).
[24] S. Longhi, M. Marangoni, M. Lobino, R. Ramponi, P. Laporta, E. Cianci, and V. Foglietti, Phys. Rev. Lett. **96**, 243901 (2006); S. Longhi, Laser and Photon. Rev. **3**, 243 (2009).
[25] V. Spiridonov and A. Zhedanov, Methods Appl. Anal. **2**, 369 (1995); Ann. Phys. (NY) **237**, 126 (1995); S. N. M. Ruijsenaars, J. Nonlinear Math. Phys. **8**, 106 (2001).
[26] A. A. Sukhorukov, Opt. Lett. **35**, 989 (2010).
[27] S. Longhi, Phys. Rev. A **82**, 032111 (2010).
[28] A. Szameit, F. Dreisow, M. Heinrich, S. Nolte, and A. A. Sukhorukov, Phys. Rev. Lett. **106**, 193903 (2011).
[29] S. Longhi, Phys. Rev. B **77**, 195326 (2008).
[30] G. Della Valle, S. Longhi, P. Laporta, P. Biagioni, L. Duò, and M. Finazzi, Appl. Phys. Lett. **90**, 261118 (2007).